Acetylcholine Receptor Gating at Extracellular Transmembrane Domain Interface: the "Pre-M1" Linker

Prasad Purohit and Anthony Auerbach

Department of Physiology and Biophysics, State University of New York at Buffalo, Buffalo, NY 14214

Charged residues in the β10–M1 linker region ("pre-M1") are important in the expression and function of neuromuscular acetylcholine receptors (AChRs). The perturbation of a salt bridge between pre-M1 residue R209 and loop 2 residue E45 has been proposed as being a principle event in the AChR gating conformational "wave." We examined the effects of mutations to all five residues in pre-M1 (positions M207–P211) plus E45 in loop 2 in the mouse α_1-subunit. M207, Q208, and P211 mutants caused small (approximately threefold) changes in the gating equilibrium constant (K_{eq}), but the changes for R209, L210, and E45 were larger. Of 19 different side chain substitutions at R209 on the wild-type background, only Q, K, and H generated functional channels, with the largest change in K_{eq} (67-fold) from R209Q. Various R209 mutants were functional on different E45 backgrounds: H, Q, and K (E45A), H, A, N, and Q (E45R), and K, A, and N (E45L). Φ values for R209 (on the E45A background), L210, and E45 were 0.74, 0.35, and 0.80, respectively. Φ values for R209 on the wt and three other backgrounds could not be estimated because of scatter. The average coupling energy between 209/45 side chains (six different pairs) was only −0.33 kcal/mol (for both α subunits, combined). Pre-M1 residues are important for expression of functional channels and participate in gating, but the relatively modest changes in closed- vs. open-state energy caused mutations, the weak coupling energy between these residues and the functional activity of several unmatched-charge pairs are not consistent with the perturbation of a salt bridge between R209 and E45 playing the principle role in gating.

The Journal of General Physiology

INTRODUCTION

In acetylcholine receptor channels (AChRs), structural changes at two transmitter binding sites are linked with structural changes at a distant (∼60 Å) "gate" in the transmembrane domain, by brownian movement along a linear sequence of intermediate steps (a "brownian conformational wave," Auerbach, 2005; Zhou et al., 2005; Purohit et al., 2007). We, and others, seek to understand the structure and dynamics of the molecular events that connect the low affinity, nonconducting C(losed) conformation of the AChR with the high affinity, ion-conducting O(pen) conformation. This intermediate conformational ensemble forms the energy barrier that separates diliganded C and O, which is the transition region (TR) of the gating reaction.

The perturbation of a salt bridge near the interface of the extracellular domain (ECD) and the transmembrane domain (TMD) of the AChR has been suggested as being the key TR event in C↔O gating. Lee and Sine (2005) studied the interaction between residues R209 at the C terminus of the ECD (at the base of loop C, in the pre-M1 segment) and E45 in loop 2, a segment that had previously been identified as playing an important and dynamic role in gating (Chakrapani et al., 2004). They found that charge-changing mutations alone (E45R or R209Q) reduced the diliganded gating equilibrium constant (K_{eq}), but that these mutations in combination yielded AChR having almost wt-like K_{eq} values. In addition, they found that the magnitude of the coupling energy between R209Q and E45R side chains was approximately that expected for a salt bridge. Given these results and the location of these closely apposed residues (Unwin, 2005; Dellisanti et al., 2007), about halfway between the transmitter binding sites and an equatorial gate and in the center of the α-subunit, they proposed that the "principle pathway" for the propagation of the gating conformational wave is as follows, in brief: agonist binding perturbs loop C, which perturbs the R209–E45 salt bridge, which perturbs other nearby elements that are somehow linked to the pore-lining transmembrane M2 helix and the gate (Lee and Sine, 2005). Several groups have also noted that charged residues located in the pre-M1 segment in AChRs and other pentameric, ligand-gated ion channels play a significant role in expression and gating, for example in 5-HT_{3A} receptors (Hu et al., 2003), Gly receptors (Castaldo et al., 2004), $GABA_A$ receptors (Kash et al., 2004; Keramidas et al., 2006; Mercado and Czajkowski, 2006), and ACh receptors (Tamamizu et al., 1995; Lee and Sine, 2005; Xiu et al., 2005). Recently, evidence for a salt bridge between residues in pre-M1 and loop 2 was

Correspondence to Anthony Auerbach: auerbach@buffalo.edu

Abbreviations used in this paper: AChR, acetylcholine receptor; ECD, extracellular domain; REFER, rate-equilibrium free energy relationship; TMD, transmembrane domain.

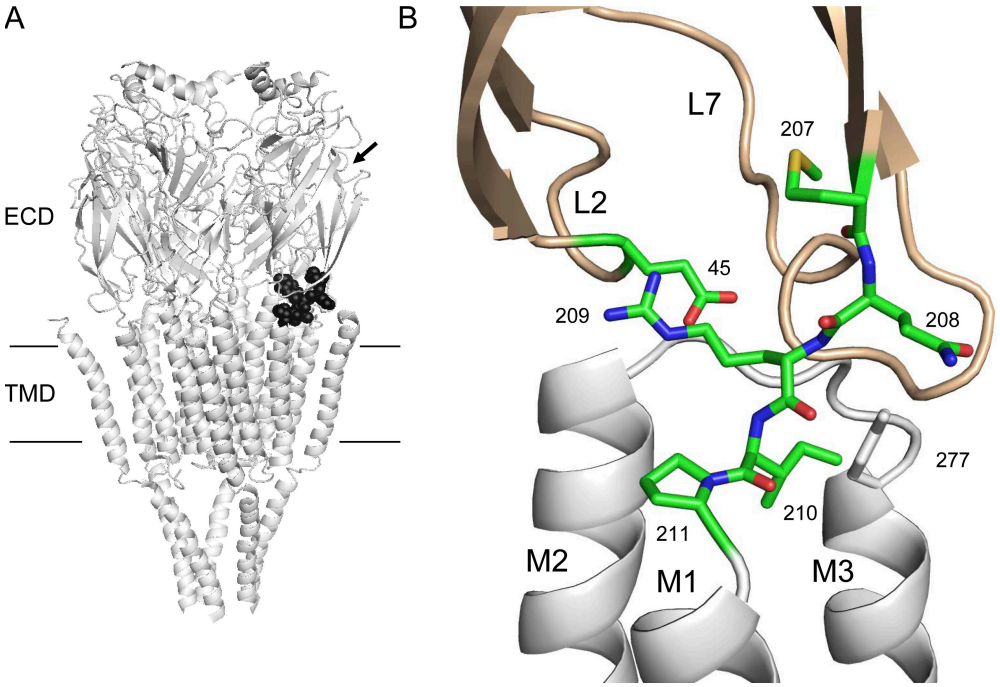

Figure 1. The AChR pre-M1 linker. (A) The *Torpedo* AChR (2bg9.pdb). The pre-M1 linker in the α_ε subunit is highlighted (black spheres). Horizontal lines and arrow mark, approximately, the membrane and the transmitter binding site. ECD, extracellular domain, TMD, transmembrane domain. (B) The five pre-M1 residues, between β-strand 10 in the ECD (tan) and M1 in the TMD (gray), plus residue E45 in loop 2 are colored by element (carbon, green; nitrogen, blue; oxygen red). For clarity, loop 9 and M4 are not shown. L7 is loop 7 (the "cys-loop") and L2 is loop 2. The pre-M1 sequence (positions 207–211) for *Torpedo* is MQRIP. Position 210 is L in mouse. Structures were displayed by using PYMOL (DeLano Scientific).

reported for ρ1 $GABA_A$ and $GABA_C$ receptors, but mutation of these residues in $5HT_3$ receptors mainly acts to reduce channel expression (Price et al., 2007; Wang et al., 2007).

We have modeled the conformational pathway between C and O as a linear sequence of intermediate steps, with the result that information about the relative timing of these steps can be gained from kinetic analyses (Zhou et al., 2005; Auerbach, 2007). The slope of a log–log plot of the opening rate constant vs. K_{eq} for a mutational series of a single residue is called Φ and, according to this model, implies the relative timing of that residue's gating motion (1 to 0, early to late). Lee and Sine (2005) combined the kinetic results for wt, R209Q, and E45K and E45R (but not E45A) to estimate Φ = 0.43 for this group, which places the R209–E45 perturbation near the middle of the gating reaction, after the movement of many M2 residues, including some near the gate (Φ = 0.65; Mitra et al., 2005; Purohit et al., 2007).

Here, we report the gating rate and equilibrium constants (and Φ) for AChRs having mutations in the α subunits of each of the five pre-M1 residues (position 207–211) or in E45. We made these measurements by using 68 different constructs, including AChRs having pairs of R209+E45 mutations (in both α subunits). The results show that only two of the pre-M1 residues move during gating. R209 moves relatively early, approximately at the same time as residues in loop 2 (including E45) and the cys-loop, and L210 moves relatively late, approximately in synchrony with the motion of M3 and the M2 equatorial (12' and 9') gate. However, the perturbation of pre-M1 residues R209 and L210 does not make a particularly large contribution to the overall energy of the gating reaction.

MATERIALS AND METHODS

For the details of mutagenesis, expression, electrophysiology, rate constant determination, and Φ-value analysis, see Jha et al. (on p. 547 of this issue). In brief, mouse AChR subunits were transiently expressed in human embryonic kidney fibroblast cells (HEK 293) and electrophysiolgical recordings were performed in cell-attached patch configuration (22°C, ∼−100 mV membrane potential, PBS in the bath and pipette). 0.1 μg/μl GFP was added as a marker in the transfection mixture. Agonist (acetylcholine or choline) was added to the pipette solution at a concentration that is approximately five times the closed-conformation equilibrium dissociation constant (K_d) (500 μM or 20 mM, respectively). Currents were analyzed by using QUB software (www.qub.buffalo.edu), with only the intervals within clusters of openings selected for quantitative analysis. Opening and closing rate constants were estimated from the selected interval durations by using a maximum-interval likelihood algorithm (Qin et al., 1997) after imposing a dead time of 25 μs. Φ was estimated as the slope of the rate-equilibrium free energy relationship (REFER), which is a plot of log k_o vs. log K_{eq}. Each point in the REFER represents the mean of at least three different patches. The coupling energy was calculated as $\Delta\Delta G = -RT\ln(K_{eq}^{wt} * K_{eq}^{DbI} / K_{eq}^{mutwt} * K_{eq}^{wtmut})$.

RESULTS

Fig. 1 shows the pre-M1 segment and loop 2 residue E45, in the *Torpedo* α-subunit (2bg9.pdb; Unwin, 2005). It is important to recall that this cryo-EM structure is of an unliganded-closed AChR, whereas we are investigating the diliganded-closed to diliganded-open gating reaction. There are significant conformational changes

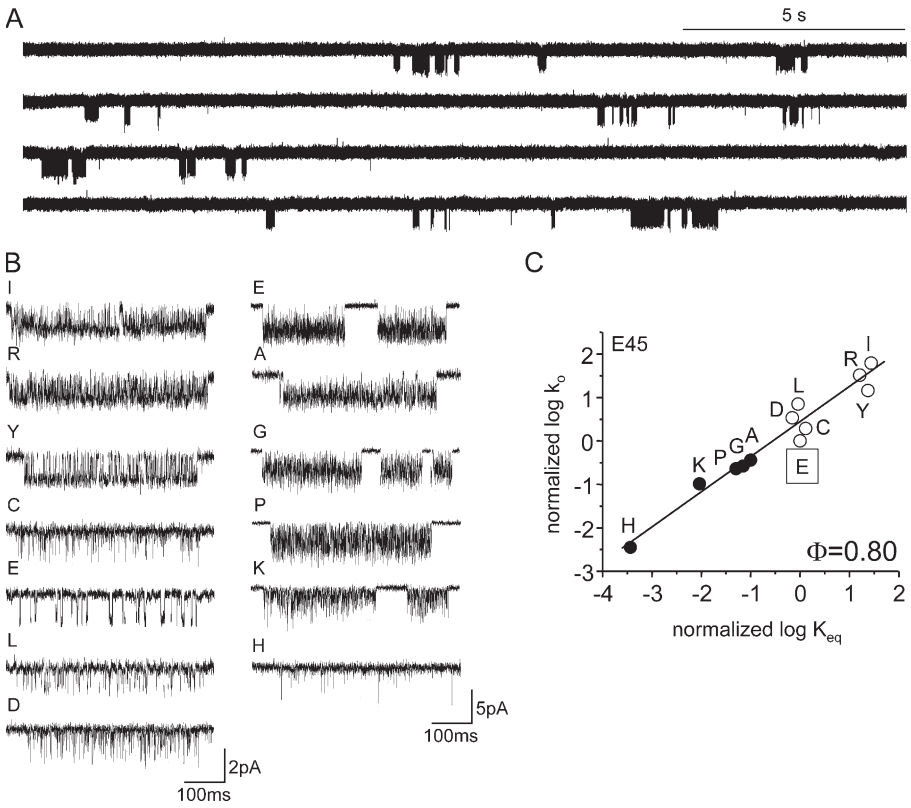

Figure 2. E45 mutational series. (A) Low time resolution view showing clusters of single-channel openings (E45R activated by choline; open is down). (B) Higher time resolution view of clusters for different side chains. Left, activated by 20 mM choline and right, activated by 500 μM ACh. The relationship between the change in the diliganded gating equilibrium constant (K_{eq}) and the chemical nature of the side chain is not simple. (C) REFER analysis. Each point represents the mean of multiple patches (Table I) (wt is boxed; filled/open circles are ACh/choline-activated). The Φ-value (bottom right) was estimated as the slope of a linear fit to a log–log plot of normalized k_o vs. normalized K_{eq} for all 10 mutants. E45 has the same Φ-value as other residues in loop 2, along with αY127 and residues in loop 7.

associated with ligand binding to AChBP (Brejc et al., 2001; Celie et al., 2004), and we therefore are uncertain the extent to which our functional results can be mapped, in detail, onto the 4-Å resolution *Torpedo* AChR structure. Also, in *Torpedo* the pre-M1 amino acid sequence is MQRIP but in mouse it is MQRLP. For both species loop 2 has the sequence EVNQ.

Fig. 2 shows a kinetic analysis of position E45 (wt plus 11 mutants). Five substitutions decreased K_{eq} (A, G, P, K, and H), three increased K_{eq} (Y, R, and I), and three had little or no effect on K_{eq} (C, D, and L). We do not discern a simple pattern relating the chemical properties of the side chain and the magnitude or polarity of the change in K_{eq}. For example, the charge reversal mutations E→K and E→R decreased and increased K_{eq}, respectively.

Regardless of whether a substitution at position 45 increased or decreased K_{eq}, the effect was to change both the opening (k_o) and closing (k_c) rate constants (Table I). The L substitution modestly increased both k_o and k_c relative to the wt and therefore had little effect on K_{eq}. A REFER plot for the entire mutant series yields $\Phi = 0.80 \pm 0.06$ (Fig. 2 B), which is the same as that for other loop 2 residues ($\Phi = 0.81 \pm 0.05$, Chakrapani et al., 2004). Separate analyses of constructs activated either by ACh or choline gave similar Φ values (0.81 ± 0.08 and 0.77 ± 0.20, respectively). (Note that the higher SEM with choline can be attributed to the smaller excursion in K_{eq} realized with this agonist.)

Next, we measured Φ values for all of the residues in α-subunit pre-M1 linker. At three positions (207, 208, and 211) none of the 11 tested mutations changed K_{eq} by about greater than threefold (Table II). The specific constructs were M207→A, G, I, W, Q208→A, E, W, and P211→A, G, H, S. This result indicates that there is a little or no difference in energy between the C vs. O conformations of these residues, which implies that the atoms do not move in the gating reaction, that they move in register with their local microenvironments or that there are compensating energy changes in nearby residues associated with their motion. The lack of a change in K_{eq} upon mutation of P211, at the top of the M1 helix, is particularly notable.

Some mutations of the two central pre-M1 residues, R209 and L210, changed K_{eq} by greater than threefold. We examined 19 different substitutions at R209, plus a construct in which residue 209 was deleted. In 16 of these (A, C, D, E, F, G, I, L, M, N, P, S, T, V, W, Y, and the deletion) no single channel currents were observed (3–10 patches/mutant, ~20 min/patch). We conclude that these constructs either fail to express or express AChRs that fail to function in a manner consistent with the time resolution of the patch clamp. We did record single-channel currents from the constructs R209Q and R209H, but only with some difficulty (currents observed in ~20% of patches), whereas currents for the R209K mutant were observed in virtually every patch. Thus, a major effect of mutating R209 is to reduce or abolish the expression of functional AChRs.

TABLE I

Kinetic Analysis of E45 Mutants

Construct	Agonist	k_o (s^{-1})	k_c^{obs} (s^{-1})	k_c^{cor} (s^{-1})	K_{eq} (k_o/k_c^{cor})	Normalized K_{eq} (mut/wt)	*n*
wt	ACh	48000	–	1700	28.2	1	–
wt	Cho	120	–	2583	0.046	1	–
E45I	Cho	7446 (377)	2235 (383)	5967 (1772)	1.3 (0.31)	28.3	3
E45Y	Cho	1736 (64)	594 (54)	1585 (251)	1.1 (0.25)	24	3
E45R	Cho	3901 (76)	1937 (32)	5172 (170)	0.76 (0.05)	16.5	4
E45L	Cho	201 (26)	1420 (176)	3791 (665)	0.05 (0)	1.2	2
E45C	Cho	856 (83)	7780 (1307)	20770 (6045)	0.043 (0.02)	0.93	3
E45D	Cho	409	4741	12650	0.03	0.65	1
E45A	ACh	17450 (715)	5060 (625)	6324 (1563)	2.91 (0.8)	0.1	4
E45G	ACh	12760 (923)	5158 (534)	6448 (1156)	2.1 0.65)	0.074	3
E45P	ACh	11040 (202)	6212 (393)	7765 (982)	1.43 (0.13)	0.05	4
E45K	ACh	4979 (352)	15390 (1149)	19240 (2871)	0.27 (0.07)	0.01	4
E45H	ACh	214 (101)	13210 (595)	16510 (744)	0.013 (0.007)	0.005	3

All values are mean ± SEM. k_o, opening rate constant; k_c^{obs}, observed closing rate constant; k_c^{cor}, closing rate constant corrected for channel-block; K_{eq} ($=k_o/k_c^{cor}$), diliganded gating equilibrium constant, normalized K_{eq} (mutant divided by the wt value for the salient agonist); *n*, number of patches.

Fig. 3 A and Table III show k_o, k_c, and K_{eq} values for the Q, H, and K substitutions of R209. The kinetic pattern was complex. The Q mutation reduced k_o by ∼7.6-fold and increased k_c by ∼9.5-fold, leading to a ∼67-fold decrease in K_{eq}. This result is similar to the 46-fold increase in K_{eq} previously reported by Lee and Sine (2005). The H substitution increased both k_o and k_c (each by ∼2.5-fold) so that there was essentially no change in K_{eq}. The K substitution also increased both k_o (15-fold) and k_c (only by 2.3-fold), leading to a modest ∼7-fold increase in K_{eq}. Overall, the REFER for R209 on the wt background showed a high degree of scatter and the Φ-value could not be estimated with a high degree of precision (0.72 ± 0.16).

We also examined the kinetics of R209 mutants using AChRs having a distant background mutation that specifically slows channel closing. δL265 is located in the M2 helix of the δ-subunit, and when this residue is mutated to a T, k_c decreases by ∼16-fold but k_o remains unchanged (Table III; Cymes et al., 2002). We used this mutant as a background construct, in combination with αR209 mutants. As with the wt background, no currents were apparent with the R209A, C, W, N, L, Y, F, and E constructs, but, as was the case with the wt background, were present with H, K, and Q. This result suggests that it is unlikely that the lack of observable currents can be attributed to an ultrafast closing rate constant in expressed AChRs. Fig. 3 B shows the REFER plot for the R209 mutant series on the δL265T background. The overall pattern was similar to that obtained with ACh on the wt background, with the exception that there was a smaller effect on k_o for the R209H construct. The estimate of the slope of the REFER for R209 mutants on the δL265T background was again imprecise (Φ = 0.48 ± 0.19) but, because of the large standard error, was not significantly different from that obtained using the wt background. The coupling interaction energy estimated for R209/L265 mutant pairs was small (average =

TABLE II

Kinetic Analysis of M207, Q208, and P211

Construct	Agonist	k_o (s^{-1})	k_c^{obs} (s^{-1})	k_c^{cor} (s^{-1})	K_{eq} (k_o/k_c^{cor})	Normalized K_{eq} (mut/wt)	*n*
M207A	Cho	288 (25.2)	1748 (288)	4666 (1333)	0.064 (0.02)	1.5	3
M207G	Cho	175 (5.4)	1094 (187)	2922 (863)	0.063 (0.02)	1.4	3
M207I	Cho	161	966	2579	0.062	1.3	1
M207W	Cho	151 (13)	495 (81)	1318 (435)	0.12 (0.02)	2.6	4
Q208A	Cho	121	423	1129	0.11	2.3	1
Q208E	ACh	ND	ND	ND	ND	ND	–
Q208W	Cho	40	800	2136	0.02	0.43	1
P211G	ACh	31402	2883	3604	8.7	0.3	1
P211H	ACh	ND	ND	ND	ND	ND	–
P211A	ACh	29000 (999)	2601 (257)	3251 (453)	8.9 (0.8)	0.3	2
P211S	ACh	36500	2450	3063	11.9	0.4	1

All of the mutants at positions M207, Q208, and P211 expressed and exhibited wt-like kinetic properties (change in K_{eq} less than threefold). ND, no data at 20 mM choline or 500 μM ACh. At 30 μM ACh both Q208E and P211H had wt-like kinetic behaviors.

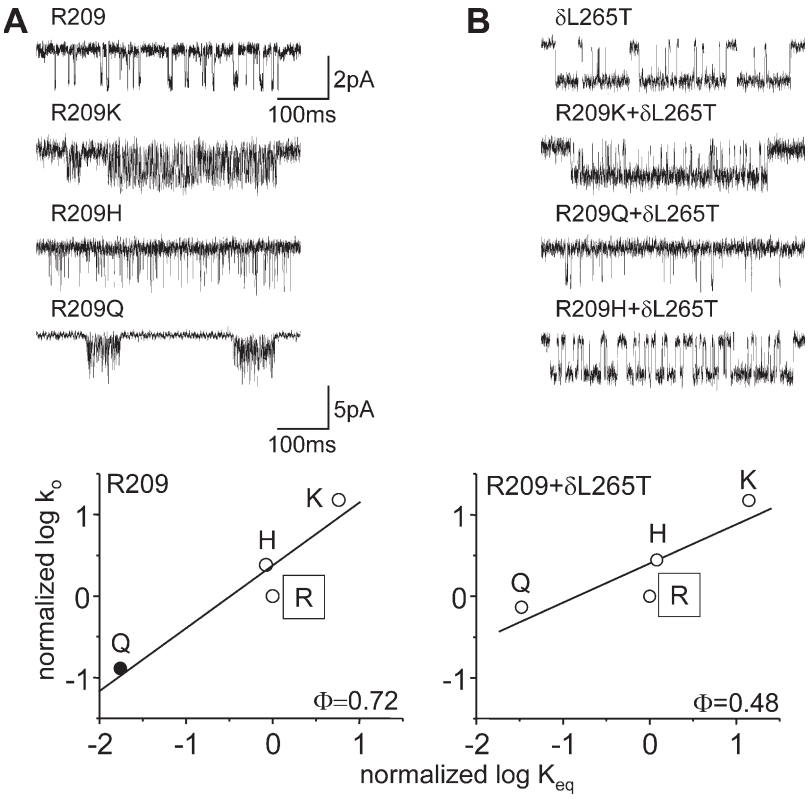

Figure 3. R209 mutational series. (A) R209 mutants on a wt background. Top, example single-channel clusters activated by choline or ACh. Single-channel currents were not detected for R209A, C, D, E, F, G, I, L, M, N, P, S, T, V, W, Y, and the deletion mutant. Bottom, each point in the REFER plot represents the mean of multiple patches (Table III); wt is boxed. The error limit on Φ (bottom right) was large (±0.16). (B) R209 mutants on the δL265T background that specifically slows channel closing. Top, example single-channel clusters activated by choline. Bottom, REFER plot. The error limit on Φ was large (±0.19)

−0.40 kcal/mol), suggesting that the effects of the two mutations were essentially independent (Table III).

The second mutation-sensitive position in pre-M1 was L210 (Fig. 4 and Table IV). At this position all of the tested mutants (Y, A, F, W, and G) expressed functional AChRs that showed an increased K_{eq} (by 2-, 6.1-, 6.3-, 10.7-, and 52.1-fold, respectively). The effect of the mutations was mainly to slow k_c, and a REFER plot for the L210 mutant series gives $\Phi = 0.35 \pm 0.12$ (Fig. 4 B). The A construct appeared to be an "outlier," but eliminating this point from the fit only reduced the standard error and did not significantly change the estimate of Φ (0.36 ± 0.07).

In the next set of experiments we measured k_o, k_c, and K_{eq} in AChRs having two mutations in each of the two α subunits. Lee and Sine (2005) used this approach to detect a significant energetic interaction (−3.1 kcal/mol) between R209Q and E45R, which supported their proposal that these two side chains (Q/R) interact during gating. We measured k_o and k_c for R209 mutants on three different mutant E45 backgrounds, R, L, and A (Fig. 5). By themselves these background mutations increase, do not change, or decrease K_{eq}, respectively (Fig. 2).

Interestingly, the expression of functional R209 mutant channels was influenced by the side chain at the background position 45. The constructs R209A and R209N are totally silent in the wt E45 background, but give rise to functional channels in the E45R and E45L backgrounds. R209A, L, and N, however, still did not generate functional channels on the E45A background.

The coupling energies between the R209 and E45 mutants are shown in Table III. In four of the tested 209/45 mutant pairs (Q/A, H/A, Q/R, and K/L) the observed value for K_{eq} was smaller than that predicted assuming independent energetic effects of the mutations. In the H/R and K/A pairs, K_{eq} was larger than predicted from independence. The magnitude of the discrepancy varied with the side chains. The degree of coupling was largest for the K/A, Q/R, and H/R pairs, for which the observed value of the normalized K_{eq} was 20.1-fold larger, 7.1-fold larger, and 6.1-fold smaller and than predicted from independence. These translate to coupling energies of −1.77, +1.16, and −1.07 kcal/mol, respectively. Overall, the average (±SD) coupling between all six different R209 and E45 mutant pairs was modest, -0.33 ± 1.02 kcal/mol.

The R209 REFERS on the E45 mutant backgrounds are shown in Fig. 5. As with the wt background, there was a large amount of scatter in the REFERs for the E45R background ($\Phi = 1.49 \pm 0.23$) and E45L background ($\Phi = 1.0 \pm 0.26$), and Φ values could not be estimated precisely. This result suggests that mutations of R209 on the wt and these backgrounds alter one or more of the TR barriers (a "catalytic" effect), that a point mutation of R209 changes the energies of multiple microstates of the TR to relative extents that depend on the specific side chain substitution, or both. Only the four-point REFER for the E45A background was clearly linear. For this construct, $\Phi = 0.74 \pm 0.02$, a value that

TABLE III

Kinetic Analysis of R2

Construct	Agonist	k_o (s^{-1})	k_c^{obs} (s^{-1})	k_c^{cor} (s^{-1})	K_{eq} (k_o/k_c^{cor})	Normalized K_{eq} (mut/wt)		ΔΔG (kcal/mol)	*n*
						Observed	Predicted		
R209Q	ACh	6288 (694)	12860 (1688)	16070 (3654)	0.42 (0.17)	0.015	–		3
R209K	Cho	1820 (149)	2197 (260)	5865 (980)	0.32 (0.09)	6.9	–	–	2
R209H	Cho	222 (54)	2614 (193)	6979 (894)	0.037 (0.007)	0.8	–	–	3
R209Q+δL265T	Cho	92.2 (18.6)	1394 (294)	3723 (1360)	0.028 (0.02)	0.63	4.1	−0.54	3
R209K+δL265T	Cho	1805 (196)	64.5 (6.5)	172 (25)	10.7 (3.13)	233	112.5	−0.42	2
R209H+δL265T	Cho	335.3 (24.5)	138.1 (9.3)	369 (43)	0.92 (0.2)	20	19.6	−0.25	3
δL265T	Cho	120	60	160	0.75	16.3	–	–	1
R209A+E45L	Cho	497.8 (64.8)	5590 (350)	14930 (1869)	0.034 (0.01)	1.4	–	–	4
R209K+E45L	Cho	976 (54)	1494 (152)	3988 (572)	0.25 (0.02)	5.4	7.9	−0.19	2
R209N+E45L	ACh	4536	2005	2506	1.8	0.06	–	–	1
R209Q+E45A	ACh	1427 (181)	16230 (1293)	20290 (3233)	0.07 (0.02)	0.002	0.00152	−0.28	4
R209K+E45A	Cho	2061 (231)	1238 (192)	3305 (886)	0.66 (0.2)	14.3	0.71	−1.77	3
R209H+E45A	ACh	11410 (642)	7319 (469)	9148 (587)	1.25 (0.08)	0.044	0.083	0.37	3
R209A+E45R	ACh	26035	761	951	27.4	0.97	–	–	1
R209H+E45R	Cho	669.5 (135)	2660 (187)	7102 (706)	0.1 (0.03)	2.17	13.3	1.1	2
R209N+E45R	ACh	2105 (389)	354.5 (44.3)	443 (111)	4.7 (0.6)	0.17	–	–	4
R209Q+E45R	Cho	513 (75)	2383 (227)	6362 (606)	0.08 (0.01)	1.74	4.1	−1.16	3

R209A, C, W, N, L, Y, F, and E did not express functional AChRs in both the wt and δL265T backgrounds. For the doubly mutated (at positions 209 and 45) α-subunit constructs, "Predicted" is the expected, normalized K_{eq} assuming that the effects of the mutations were independent. The coupling energy was calculated as described in the Materials and methods.

is similar to Φ for E45 and other loop 2 residues on the wt background.

We also examined the energetic coupling between side chains at pre-M1 residue L210 and M3 residue Y277. These side chains are close (<4 Å) in the *Torpedo* AChR structure (Fig. 1). The Φ-value for Y277, which is at the top of M3, is 0.34 (Cadugan and Auerbach, 2007) and about the same as for L210. Two double mutant 210/277 pairs were examined (G/H and W/H; Table IV). Based on the observed and the predicted K_{eq} values, these two side chains show little coupling (0.69 and 0.54 kcal/mol, respectively), which is surprising given that they are so closely apposed in the *Torpedo* AChR structure. These results indicate that the energetic consequences of mutating L210 and Y277 are approximately independent.

DISCUSSION

Comparison with Previous Results

There are three major differences between our results and those of Lee and Sine (2005), who also studied mutants of αR209 and αE45. First, we find that E45 has an Φ-value (0.80) that is same as those for other loop 2 residues (0.81), as well as for many cys-loop residues (0.78). Using the rate constants reported in Lee and Sine (2005), we calculate an Φ-value for E45 (0.44 ± 0.12; for the wt and A, K, and R mutants) that is lower than our estimate. Second, with choline as the agonist we find that the charge-reversal mutation E45R causes an ∼16.5-fold increase in K_{eq}, whereas Lee and Sine used ACh as the agonist and found that this mutation caused a 6.6-fold decrease in K_{eq}. Xiu et al., (2005) found that in mouse AChRs (expressed in *Xenopus* oocytes) the E45R mutation decreased the EC_{50} for ACh (from 50 to 1.6 μM), which is consistent with our observation of an increase in K_{eq}. This result, and those shown in Fig. 2 B, indicates that the discrepancy cannot be attributed to different agonists. Third, we find the coupling between the R209Q and E45R side chains is −1.15 kcal/mol, whereas Lee and Sine report a larger (−3.1 kcal/mol) energetic interaction for this same mutant pair. This difference in coupling energy can be traced to the essential difference with regard to the effect of the E45R mutation alone on K_{eq}.

The sources of the differences in results regarding E45 in our hands (mouse AChRs, in HEK cells, exposed to extracellular Na^+) and those of Lee and Sine (human AChRs, in BOSC23 cells, exposed to extracellular K^+) remain unknown. Note that even if the E45R data point is eliminated from the E45 REFERs a significant difference in Φ for position E45 persists (0.80 ± 0.10 vs. 0.44 ± 0.17, ours vs. Lee and Sine). Our results indicate that αE45 moves relatively early in the channel opening process, at approximately the same time as all of the other residues in loop 2 and the neighboring cys-loop, and that a charge reversal mutation at this position increases K_{eq}.

Salt Bridge Hypothesis

Although R209 and E45 are close (<4 Å) to each other in the both the *Torpedo* and mouse ECD fragment

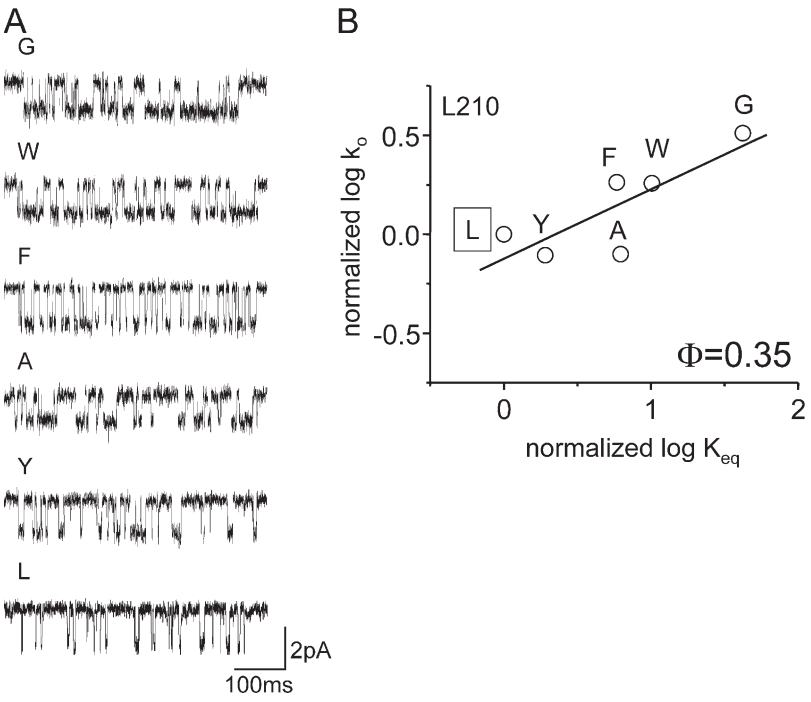

Figure 4. L210 mutational series. (A) Example clusters elicited by choline. All of the mutations increased K_{eq} and the cluster open probability, mainly by prolonging the open time (slowing the closing rate constant). (B) REFER plot (Table IV); wt is boxed. The Φ-value for L210 was $\Phi = 0.35 \pm 0.12$, which suggests that this residue moves "late" in the gating isomerization.

structures, certain results are difficult to reconcile with the hypothesis that the perturbation of a salt bridge between these side chains is a principle event in AChR gating. (a) Lee and Sine (2005) report that the mutation R209Q (in both α subunits) causes only a 46-fold reduction in K_{eq}, which is similar to our measurement of a 67-fold reduction. This degree of change in K_{eq} is significant, but smaller than others caused by the mutation of other residues that are near the base of the ECD/TMD interface and elsewhere. For example, the following mutations (also in both α subunits) all cause a larger change in K_{eq}: D97A (170-fold; Chakrapani et al., 2003), Y127D (4947-fold; Purohit and Auerbach, 2007), V46E (233-fold; Chakrapani et al., 2003), F135A (134-fold; Chakrapani et al., 2004), I274T and P272A (1613- and 218-fold, respectively; Jha et al., 2007). In addition, the mutation of several δ- (Cymes et al., 2002) and α-subunit (Mitra et al., 2004; Mitra et al., 2005; Cadugan and Auerbach, 2007; Purohit et al., 2007) TMD residues also causes a >100-fold change in K_{eq}. Although R209 and E45 each play a significant role in gating, the unspectacular changes in energy (O vs. C) caused by R209 mutations are not consistent with this residue playing the principle role in AChR gating. (b) Charge-changing mutations do not have the expected effects for the perturbation of a salt bridge. In our hands, the charge-reversal mutation E45R increases K_{eq} while the charge-reversal mutation E45K decreases K_{eq}. Substitution of a neutral side chain at E45 can either increase (I), decrease (A), or have essentially no effect (L). Likewise, at R209 the substitution of an H (which is probably uncharged at pH 7.4 when buried in a protein) has almost no effect

TABLE IV
Kinetic Analysis of L210

Construct	Agonist	k_o (s^{-1})	k_c^{obs} (s^{-1})	k_c^{cor} (s^{-1})	K_{eq} (k_o/k_c^{cor})	Normalized K_{eq} (mut/wt) Observed	Predicted	ΔΔG (kcal/mol)	*n*
L210G	Cho	408 (91)	78 (15)	207 (70)	2.4 (1.7)	52.1	–	–	3
L210W	Cho	220 (21)	176 (22)	471 (117)	0.49 (0.2)	10.7	–	–	4
L210A	Cho	96 (8)	124 (8.5)	331 (39)	0.29 (0.009)	6.3	–	–	3
L210F	Cho	225 (30)	316 (55)	845 (294)	0.28 (0.06)	6.1	–	–	4
L210Y	Cho	106 (28)	424.4 (80)	1133 (475)	0.09 (0.04)	2	–	–	5
Y277H[a]	Cho	43	7539.4	20130.2	0.0021	0.046			
L210G+Y277H	Cho	73 (4)	834 (1456)	2226 (549)	0.034 (0.01)	0.74	2.39	0.69	2
L210W+Y277H	Cho	24.7 (4)	1115 (175)	2976 (809)	0.009 (0.005)	0.19	0.49	0.54	3

The expression of all the mutants was approximately normal. The coupling energies between the mutant pairs (G/H and W/H at positions 210/277) were calculated as described in the Materials and methods.

[a]Cadugan and Auerbach (2007) and rate constant are translated for wt background.

on K_{eq}. Further, the double mutant R209A+E45L, which does not have a charged side chain at either position, has a K_{eq} that is nearly normal. Similarly, the R209/E45 constructs H/A, N/L, K/L, H/R, A/R, N/R, and Q/R cannot form such a salt bridge but nonetheless are functional. The relationship between K_{eq} and the chemical nature of the 209/45 side chain is not consistent with the perturbation of a salt bridge being the chemical interaction between these two positions. (c) We observe weak energetic coupling between some 209/45 side chains. Specifically, the average coupling energy was not significantly different from zero for the six double mutant constructs. In summary, the magnitudes of the changes in K_{eq}, the magnitudes of the coupling energies, and the pattern of change as a function of side chain chemistry are not consistent with the perturbation of a salt bridge between R209 and E45 being an energetically dominant event in AChR gating.

Primary Roles for R209

Lee and Sine (2005) reported in human AChRs that R209Q, but not R209E, gave functional expression of surface channels. Tamamizu et al. (1995) found in *Torpedo* AChRs that R209K and H mutants produce currents but L, A, and E mutants do not, and that α-bungarotoxin binding is reduced by approximately threefold in these three nonfunctional constructs. Vicente-Agullo et al. (2001) found that there was no internal or surface expression of R209L bovine α_7 receptors, and that the surface expression of bovine α_3 AChRs was attenuated by R209A and R209E (but not R209K) mutations. Xiu et al. (2005) also found that in the mouse α_1 subunit the R209A construct did not express on the surface of oocytes. We examined 19 different mutants of R209 and 11 different mutants of E45 and a striking result was that only three of the R209 point mutants (Q, H, and K) gave rise to functional channels whereas all of the E45 mutants did so. Such a general failure to express functional channels following a point mutation is rare. We did not measure surface expression, but our results are consistent with the idea that R209 is important in AChR assembly and expression, as is the case with $5HT_3$ receptors (Price et al., 2007). Because we were able to record functional R209A and N mutant channels only on the E45 R and L mutant backgrounds, we speculate that R209–E45 interactions may be important in this regard.

K_{eq} and Φ

In the five pre-M1 residues that we examined none of the 26 mutants at positions M207, Q208, and P211 changed K_{eq} (but all gave rise to functional channels). In contrast, of the constructs that produced functional channels, most at positions R209 and E45 changed K_{eq} by greater than threefold. This result suggests that α-subunit residues 207, 208, and 211 probably do not move (or move with their environment) between C and O, and that in pre-M1 only positions R209 and L210 move in the TR of the diliganded gating reaction. Compared with other domains that are also in the vicinity of the ECD–TMD

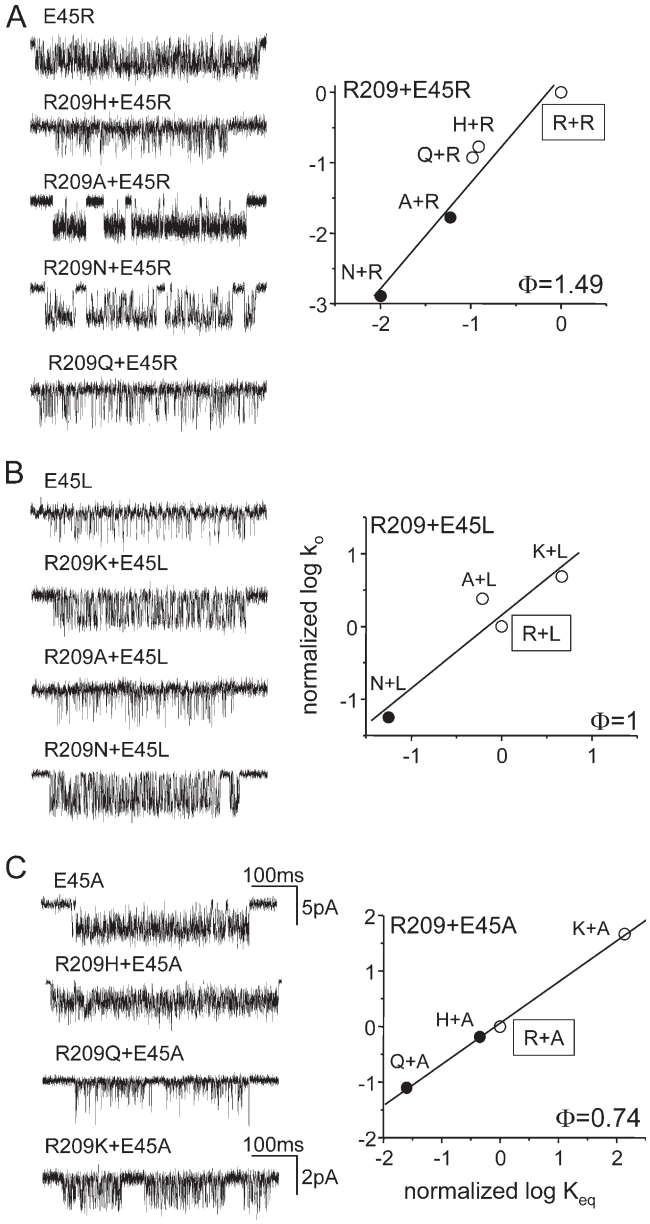

Figure 5. Energy coupling between R209 and E45. Example currents and REFERs for R209 mutations series on three different E45 backgrounds: (A) E45R, (B) E45L, and (C) E45A (Table III). Mutations were made at both R209 and E45 (in both α subunits) and current was activated by choline (open circles) or ACh (filled circles). The R209A and R209N point mutants in a wt background did not yield functional AChRs but did so in the E45R and E45L backgrounds. The Φ values estimated for position 209 in E45R and E45L backgrounds are imprecise because of a large SD (±0.23 and ±0.26). A mutant cycle analysis for these constructs indicates that the coupling between R209K/45A, R209Q/E45R, and R209H/E45R is greater than between R209Q/E45A and R209K/E45L (Table III). The REFER for R209 on an E45A background was linear over a greater than three order of magnitude range in K_{eq}, and is our best estimate of the Φ-value for R209.

interface (for example, the M2–M3 linker, the cys-loop and loop 2), the pre-M1 segment does not appear to make major contribution to the energy difference between C and O. Rather, we think that the transfer of energy between the ECD and TMD is mediated to a greater extent by a combination of side chain interactions at multiple sites between loop 2 and M2, and between the cys-loop and the M2–M3 linker. Such a distributed nature for these interactions is consistent with the general observation that relationship between the chemical nature of a single amino acid and the change in K_{eq} is rarely simple.

It is interesting that the REFERs for the two moving residues in pre-M1 (R209 and L210) were scattered. For R209, we measured Φ values (on five different backgrounds) ranging from 0.48 to 1.49, and with SEM values that ranged from 0.02 to 0.26. For L210, the standard error of the Φ estimate was 0.35 ± 0.12. For comparison, the SEM values for 14 different M2 residue REFERs (over a similar spread in K_{eq}) ranged from 0.01 to 0.16 (Purohit et al., 2007). We are not sure why the REFERs for R209 are so problematic. We note that R209 and L210 are in a region that is characterized by several different Φ values, including loop 2 and the cys-loop (Φ ≈ 0.78), the M2–M3 linker (Φ ≈ 0.64), and M3 (Φ ≈ 0.31). Given this location, at the junction of three "nanotectonic plates," we speculate that some mutations of R209 perturb multiple positions of the TR. If the relative extents of these energy perturbations vary with the side chain substitution, then the REFERs would be scattered.

The REFER for R209 on an E45A background was linear (over a greater than three order of magnitude range in K_{eq}) and showed little scatter, and thus gave rise to a reliable estimate for Φ. This estimate, 0.74 ± 0.02, is similar to the one obtained on the wt background, 0.72 ± 0.16, so it is the best estimate of the Φ-value for R209. This value places the gating motion of R209 relatively early in the gating reaction, approximately in synchrony with α-subunit residues in loop 2 (including E45) and the cys-loop, and residue Y127. This value also places R209 at a Φ-block boundary, because the Φ-value of its neighbor, L210, is only 0.35.

The REFER for E45 (Φ = 0.77; Fig. 2) spanned an ∼35,805-fold range in K_{eq} value (E45H to E45R), which indicates that the movements of this residue (in two α subunits) is important insofar as this side chain substitution results in a significant (−6.18 kcal /mol) energetic contribution to the gating equilibrium constant. However, we can discern no simple pattern relating the value of K_{eq} to the chemical nature of the side chain at this position.

Regarding position L210, all five of the tested mutants gave rise to functional channels in which K_{eq} was increased relative to the wt. The Φ-value for L210 (0.35) suggests that this residue is part of a domain that moves late in the reaction and whose motion links the ECD–TMD interface with those in M3 near the middle of the membrane. There is only a small degree of energetic coupling between L210 and Y277 side chains, even though these residues are closely apposed in the *Torpedo* structure. We do not yet understand the physiological significance of residues at the ECD–TMD interface moving late in the gating reaction, perhaps with or even after the change in ionic conductance at the gate (Purohit et al., 2007). We speculate that these late gating motions may serve as a "latch" that stabilizes the O conformation of the protein.

We would like thank Mary Merritt and Mary Teeling for technical assistance.

Olaf S. Andersen served as editor.

Submitted: 17 July 2007
Accepted: 8 November 2007

REFERENCES

Auerbach, A. 2005. Gating of acetylcholine receptor channels: Brownian motion across a broad transition state. *Proc. Natl. Acad. Sci. USA.* 102:1408–1412.

Auerbach, A. 2007. How to turn the reaction coordinate into time. *J. Gen. Physiol.* 130:543–546.

Brejc, K., W.J. van Dijk, R.V. Klaassen, M. Schuurmans, J. van Der Oost, A.B. Smit, and T.K. Sixma. 2001. Crystal structure of an ACh-binding protein reveals the ligand-binding domain of nicotinic receptors. *Nature.* 411:269–276.

Cadugan, D.J., and A. Auerbach. 2007. Conformational dynamics of the αM3 transmembrane helix during acetylcholine receptor channel gating. *Biophys. J.* 93:859–865.

Castaldo, P., P. Stefanoni, F. Miceli, G. Coppola, E.M. Del Giudice, G. Bellini, A. Pascotto, J.R. Trudell, N.L. Harrison, L. Annunziato, and M. Taglialatela. 2004. A novel hyperekplexia-causing mutation in the pre-transmembrane segment 1 of the human glycine receptor α1 subunit reduces membrane expression and impairs gating by agonists. *J. Biol. Chem.* 279:25598–25604.

Celie, P.H., S.E. van Rossum-Fikkert, W.J. van Dijk, K. Brejc, A.B. Smit, and T.K. Sixma. 2004. Nicotine and carbamylcholine binding to nicotinic acetylcholine receptors as studied in AChBP crystal structures. *Neuron.* 41:907–914.

Chakrapani, S., T.D. Bailey, and A. Auerbach. 2003. The role of loop 5 in acetylcholine receptor channel gating. *J. Gen. Physiol.* 122:521–539.

Chakrapani, S., T.D. Bailey, and A. Auerbach. 2004. Gating dynamics of the acetylcholine receptor extracellular domain. *J. Gen. Physiol.* 123:341–356.

Cymes, G.D., C. Grosman, and A. Auerbach. 2002. Structure of the transition state of gating in the acetylcholinereceptor channel pore: a Φ-value analysis. *Biochemistry.* 41:5548–5555.

Dellisanti, C.D., Y. Yao, J.C. Stroud, Z.Z. Wang, and L. Chen. 2007. Crystal structure of the extracellular domain of nAChR α1 bound to α-bungarotoxin at 1.94 Å resolution. *Nat. Neurosci.* 10:953–962.

Hu, X.Q., L. Zhang, R.R. Stewart, and F.F. Weight. 2003. Arginine 222 in the pre-transmembrane domain 1 of 5-HT3A receptors links agonist binding to channel gating. *J. Biol. Chem.* 278:46583–46589.

Jha, A., D. Cadugan, P. Purohit, and A. Auerbach. 2007. Acetylcholine receptor channel gating at extracellular transmembrane domain interface: the cys-loop and M2–M3 linker. *J. Gen. Physiol.* 130:547–558.

Kash, T.L., M.J. Dizon, J.R. Trudell, and N.L. Harrison. 2004. Charged residues in the β2 subunit involved in GABAA receptor activation. *J. Biol. Chem.* 279:4887–4893.

Keramidas, A., T.L. Kash, and N.L. Harrison. 2006. The pre-M1 segment of the α1 subunit is a transduction element in the activation of the GABAA receptor. *J. Physiol.* 575:11–22.

Lee, W.Y., and S.M. Sine. 2005. Principal pathway coupling agonist binding to channel gating in nicotinic receptors. *Nature.* 438:243–247.

Mercado, J., and C. Czajkowski. 2006. Charged residues in the α1 and β2 pre-M1 regions involved in GABAA receptor activation. *J. Neurosci.* 26:2031–2040.

Mitra, A., T.D. Bailey, and A.L. Auerbach. 2004. Structural dynamics of the M4 transmembrane segment during acetylcholine receptor gating. *Structure.* 12:1909–1918.

Mitra, A., G.D. Cymes, and A. Auerbach. 2005. Dynamics of the acetylcholine receptor pore at the gating transition state. *Proc. Natl. Acad. Sci. USA.* 102:15069–15074.

Price, K.L., K.S. Millen, and S.C. Lummis. 2007. Transducing agonist binding to channel gating involves different interactions in 5-HT33 and GABAc receptors. *J. Biol. Chem.* 282:25623–25630.

Purohit, P., and A. Auerbach. 2007. Acetylcholine receptor gating: movement in the α-subunit extracellular domain. *J. Gen. Physiol.* 130:569–579.

Purohit, P., A. Mitra, and A. Auerbach. 2007. A stepwise mechanism for acetylcholine receptor channel gating. *Nature.* 446:930–933.

Qin, F., A. Auerbach, and F. Sachs. 1997. Maximum likelihood estimation of aggregated Markov processes. *Proc. Biol. Sci.* 264:375–383.

Tamamizu, S., A.P. Todd, and M.G. McNamee. 1995. Mutations in the M1 region of the nicotinic acetylcholine receptor alter the sensitivity to inhibition by quinacrine. *Cell. Mol. Neurobiol.* 15:427–438.

Unwin, N. 2005. Refined structure of the nicotinic acetylcholine receptor at 4 Å resolution. *J. Mol. Biol.* 346:967–989.

Vicente-Agullo, F., J.C. Rovira, S. Sala, F. Sala, C. Rodriguez-Ferrer, A. Campos-Caro, M. Criado, and J.J. Ballesta. 2001. Multiple roles of the conserved key residue arginine 209 in neuronal nicotinic receptors. *Biochemistry.* 40:8300–8306.

Wang, J., H.A. Lester, and D.A. Dougherty. 2007. Establishing an ion pair interaction in the homomeric rho GABAa receptor that contributes to the gating pathway. *J. Biol. Chem.* 282:26210–26216.

Xiu, X., A.P. Hanek, J. Wang, H.A. Lester, and D.A. Dougherty. 2005. A unified view of the role of electrostatic interactions in modulating the gating of Cys loop receptors. *J. Biol. Chem.* 280:41655–41666.

Zhou, Y., J.E. Pearson, and A. Auerbach. 2005. Φ-Value analysis of a linear, sequential reaction mechanism: Theory and application to ion channel gating. *Biophys. J.* 89:3680–3685.